2021 43rd Annual International Conference of the
IEEE Engineering in Medicine & Biology Society (EMBC)
Oct 31 - Nov 4, 2021. Virtual Conference

Data-Limited Deep Learning Methods for Mild Cognitive Impairment Classification in Alzheimer's Disease Patients*

Ashley De Luna[1] and Roummel F. Marcia[2]

Abstract— **Mild Cognitive Impairment (MCI) is the stage between the declining of normal brain function and the more serious decline of dementia. Alzheimer's disease (AD) is one of the leading forms of dementia. Although MCI does not always lead to AD, an early diagnosis of MCI may be helpful in finding those with early signs of AD. The Alzheimer's Disease Neuroimaging Initiative (ADNI) has utilized magnetic resonance imaging (MRI) for the diagnosis of MCI and AD. MCI can be separated into two types: Early MCI (EMCI) and Late MCI (LMCI). Furthermore, MRI results can be separated into three views of axial, coronal and sagittal planes. In this work, we perform binary classifications between healthy people and the two types of MCI based on limited MRI images using deep learning approaches. Specifically, we implement and compare two various convolutional neural network (CNN) architectures. The MRIs of 516 patients were used in this study: 172 control normal (CN), 172 EMCI patients and 172 LMCI patients. For this data set, 50% of the images were used for training, 20% for validation, and the remaining 30% for testing. The results showed that the best classification for one model was between CN and LMCI for the coronal view with an accuracy of 79.67%. In addition, we achieved 67.85% accuracy for the second proposed model for the same classification group.**

I. INTRODUCTION

Mild cognitive impairment (MCI) is a condition where individuals experience a decline in their mental and cognitive abilities. It is the intermediate stage before the development of Alzheimer's disease (AD) and other types of dementia. Although MCI does not always transition into AD, an early diagnosis of MCI could benefit those individuals, their families, and governments on a social and financial level. A study found that if all AD patients were diagnosed in the early stages, it would save a total of $7 trillion to $7.9 trillion [1]. Also, once an individual is properly diagnosed with MCI, they and their family have a better timeline for social, financial and medical decisions.

MCI is the phase between pre-clinical AD and the more serious decline of dementia due to AD. A person with MCI will have symptoms evidence of Alzheimer's brain changes, such as subtle problems with mental and cognitive abilities. Other typical symptoms of those with MCI are memory loss or speech difficulties. For some, these symptoms may not interfere with everyday activities, while for others that do develop memory and cognitive issues, the brain can no longer compensate for the damage cause by AD [2].

Considering those with MCI, one study found that after two years' follow-up, 15% of individuals older than 65 have developed dementia [3]. Another study found that 32% of individuals with MCI developed Alzheimer's dementia within five years' follow-up [4]. Lastly, a third study found that individuals who were tracked for five years or more, 38% developed dementia [5]. However, there are cases where individuals with MCI revert back to normal cognition or remain stable. Current research goals focus on properly identifying individuals with MCI since they are more likely to develop AD.

MCI is divided into early MCI (EMCI) and late MCI (LMCI). Due to the similarities between healthy and MCI brain images, the classification between EMCI and normal aging brains remains a challenging and critically important problem. In this paper, we propose using machine learning techniques for classifying images from patients who potentially have MCI in a limited-data setting.

Brain imaging methods, such as magnetic resonance imaging (MRI) have become a significant tool in the diagnosis of MCI and AD. There is a morphological difference between the control normal, EMCI and LMCI in the hippocampus region of the brain that is viewed in MRI images [6]. The Alzheimer's Disease Neuroimaging Initiative (ADNI) is the database used to acquire the MRI images for this study. In addition, the statistical parameter mapping software allows us to observe the variance in brain structure and function by studying the biomarkers in brain images based on the gray matter extracted from MRI images. Then, we will use and compare two different convolutional neural networks (CNNs) to classify between individuals into control normal, EMCI or LMCI.

A big challenge in the field of machine learning is the amount of data available, especially in medical imaging, where data are often very limited. Estimating the minimum amount of data required for a model to accurately make predictions is difficult, which is why investigating the classification accuracy of MCI **in data-limited settings** is crucial.

Related work. Numerous work exists in literature on MCI classification using machine learning, including [7], [8], [9], [10], [11], [12], [13], [14]. The overview paper [15] states that machine learning approaches for predicting dementia risk is "not yet ready for routine use," but this assessment only considered methods developed between 2006 and 2016. More recent work includes [16], where a convolutional

*This work is funded in part by National Science Foundation Grant IIS 1741490.

[1]Ashley De Luna is with the Applied Mathematics Department of the University of California, Merced, 5200 N. Lake Road, Merced, CA 95343, USA adeluna3@ucmerced.edu

[2]Roummel F. Marcia is with the Applied Mathematics Department of the University of California, Merced, 5200 N. Lake Road, Merced, CA 95343, USA rmarcia@ucmerced.edu

neural network is used to perform two-dimensional MRI classification of mild cognitive impairment. In addition, there are some works that perform using a different kind of neural network for non-binary classification. For instance, in [17], Korolev et al. study three-dimensional MRI with a recurrent neural network and a CNN for multi-classification of Alzheimer's disease, mild cognitive impairment and normal brains. Furthermore, in [18], Mehmood et al. propose using a Siamese CNN for three-dimensional MRI multi-classification of Alzheimer's disease. Lastly, other related works include the classification using positron emission tomography (PET) scans instead of MRI scans, such as in [19], where Forouzannzhad et al. study the classification MCI with three-dimensional PET scans using a CNN. In this paper, we propose using two different convolutional neural networks for MRI classification with **limited two-dimensional data**, where the dataset consists of two-dimensional slices along the axial, coronal and sagittal anatomical planes.

II. Data

The data accessed for this project was acquired from the ADNI database, which is publicly available here: `http://adni.loni.usc.edu/`. Created in 2004, the ADNI database has since continued its innovation for early detection and to identify ways to track the Alzheimer's diseases progression with biomarkers. It is funded by the National Institutes of Health with the purpose to support advances in AD research.

A. Pre-processing

The format of the downloaded MRI images from the ADNI database are the Neuroimaging Informatics Technology Initiative (NIfTI) files. It is important to note that the data image types downloaded are semi-processed, meaning that the images are aligned and centered and not the original raw MRI data. This is important because the additional pre-processing in this study will not be possible on the original data since they are not properly aligned.

The MRI can be viewed as two dimensional orthogonal projections of the brain (i.e. coronal, sagittal, and axial (see Fig. 1)). The software Statistical Parametric Mapping (SPM) was used for the pre-processing of the neuroimages. For this part of the pre-processing, the most current version of SPM12 [20] in unison with MATLAB(2019b) was used. Other alternatives such as Freesurfer and Ants could have been used. The three main steps of the pre-processing are segmentation, normalization and finally smoothing.

Segmentation. The first part of the pre-processing is known as segmentation. The 3D MRI images can be classified into different tissues types. The tissue types are defined based on the tissue probability maps (TPM) provided by SPM12. This can be found in SPM - tpm/TPM.nii, which is a multivolume NIfTI file (one volume for each of the 6 tissues classes).The TPM reflect the probability of a voxel, which represents a value on a regular grid in three dimensional space, belonging to each tissue class based on the segmentation of a large number of young adult brains that have been normalized to standard space. The order of the tissue is the following: gray matter, white matter, cerebral spinal fluid, bone, soft tissues and air/background. The features in brain images used to distinguish between AD, MCI and healthy brains are gray matter, white matter and cerebrospinal fluid. For this study we will focus on gray matter. Research shows that gray matter measurements can be detected in brain alterations that are associated with cognitive impairment [21]. After segmentation, a native-space image is produced that reflect the voxel's probability of belonging to the gray matter tissue class (Fig. 2(a)).

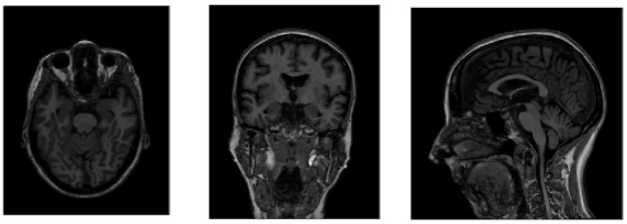

(a) Axial plane (b) Coronal plane (c) Sagittal plane

Fig. 1: Two dimensional orthogonal projection of MRI images before being preprocesed.

In order to complete segmentation through SPM12, the bias regularization is set on the light regularization (0.001), the bias full width at half maximum is set on the 60 mm cutoff, and the affine regularization on the International Consortium of Brain Mapping space template. Lastly, for the spatial normalization of the data to the Montreal Neurological Institute (MNI) spaces, the deformation field was set in the forwarding mode.

Normalization. After segmentation, the GM images were further analyzed with the next step (normalization), as seen in Fig. 2(b). Before SPM12, spatial normalization was based on minimizing the mean squared difference between a template and a warped version of the image. Now, spatial normalization involves warping all the segmented images to the same space, which is achieved by matching to a common template. The TPM defines the space that the segmented images will be warped to. This process produces a deformation field image file (y_*.nii), which records the non-linear transformation between spaces. During the non-linear transformation, it is calculated how the image should move and shrink or expand to fit the template. Thus, the deformation field contains three image volumes encoding the x, y, and z coordinates (in mm) of where each voxel maps to in the standard space. In order to normalize the GM images to MNI space, we set the written normalized images voxel size on $2 \times 2 \times 2$ mm and the interpolation to the 4th Degree B-Spline.

Smoothing. The final pre-processing step is smoothing (Fig. 2(c)), which is completed in order to increase signal to noise ratio (SNR) and the ability of statistical techniques to detect true and task related changes in the signal. All normalized GM images were set with the Gaussian smoothing kernel set to $2 \times 2 \times 2$ mm.

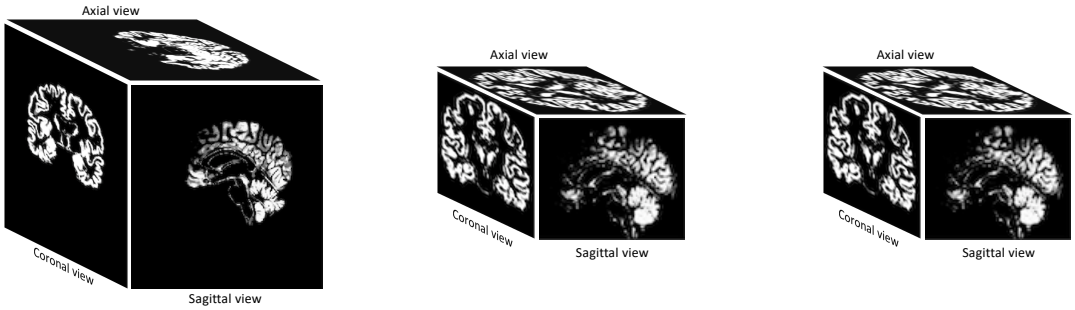

(a) Segmentation (b) Normalization (c) Smoothing

Fig. 2: The three pre-processing phases.

The original size of the data was $176 \times 240 \times 256$. After segmentation the dimensions of the image remain the same. Then, after the normalization process, all the GM images were reduced to the size of $79 \times 95 \times 79$. The dimensions were reduced but the amount of information is retained. In particular, the pixel resolution of the images were not downsampled. Rather, empty spaces that did not contain any information were excised.

B. 2D MRI Data

Now, the preprocessed 3D MRI NIfTI images are sliced into 2D portable network graphics (PNG) images for the model using MATLAB (2019b). We sliced the 3D MRI images into 2D MRI images along the three planes: axial, coronal and sagittal planes and resized them to 64×64 pixels to be used for the convolutional neural network.

Depending on the anatomical plane, we consider what we believe is the appropriate range of slices of the brain for the model. For example, in the axial plane, the top and bottom portion of the brain will not show a significant difference between healthy brains and those with MCI. Also, in the coronal plane and sagittal plane, the same consideration is applied for the front/back and left/right sides of the brain, respectively. Since we want to study the classification of MCI under data limitations, we choose a small range of images per plane. Therefore, we selected 20 images of each plane; a total of 60 images were considered per subject. The respective slices for each plane are shown in Fig. 3 through the various anatomical plane points-of-view (PoV). We make the assumption that this range of images will allow us to appropriately differentiate between CN, EMCI and LMCI.

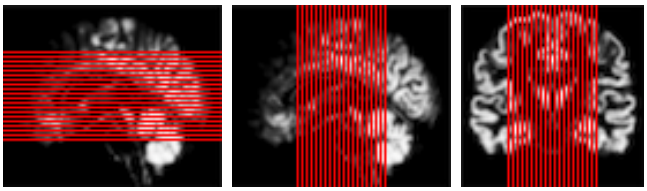

(a) Axial slices from sagittal plane PoV (b) Coronal slices from sagittal plane PoV (c) Sagittal slices from coronal plane PoV

Fig. 3: MRI image slices from various points-of-view (PoV).

C. Patient Data

For this study, we obtained a total of 516 subjects: 172 EMCI, 172 LMCI and 172 control normal subjects. The demographic information of all the subjects of the three groups are shown in Table I, where F and M are the number of females and males, respectively.

TABLE I: Demographic charateristic of the 172 subjects for each group.

	Control Normal 90 F / 82 M		Early MCI 76 F / 96 M		Late MCI 77 F / 95 M	
Age	Mean	SD	Mean	SD	Mean	SD
	76.1	6.9	71.3	7.7	72.3	7.5

Then, 10,320 images were used from each of the three planes: axial, coronal and sagittal from each group (CN, EMCI, and LMCI) for a total of 36,000 images used in the study. Additionally, the images were separated as 50% images used for training, 30% images used for testing and 20% images used for the validation set.

III. PROPOSED APPROACHES

In this paper, we performed a binary classification between Control Normal (CN), Early MCI (EMCI), and Late MCI (LMCI) within each of the axial, coronal and sagittal planes. We applied deep learning approaches that used two different convolutional neural network models described in the following sections The parameter values used in the CNNs are standard values for the given image sizes.

A. Model I: Simple CNN

The first model we considered is a variation of the model found in [16]. It is composed of three convolutional layers with max pooling between each layer. For the first convolutional network, the 32 filters with a kernel size of 3×3 and a max-pooling kernel size set on 2×2 were considered. The second and third layer consists of 128 and 512 filters respectively, followed by the same max-pooling kernel size from the first layer. Throughout all the convolutional layers, ReLU was used as the activation function. Then, a fully connected network with 128 input neurons and a ReLU activation function was used. Finally, a sigmoid activation function was used to conduct the binary classification. The

model is compiled with the Adam optimizer [22] with a learning rate of 1×10^{-4}. A binary cross entropy function was used to measure the performance of the model. The batch size was set to 128 images and used 100 epochs for the CNN.

B. Model II: VoxCNN

For the second model, we considered the VoxCNN in two-dimension, which is similar to the model found in [17]. This model is composed of four volumetric convolutional blocks of 8, 16, 32 and 64 filters, followed by the same max pooling in between, along with ReLU used as an activation function. After, a fully connected network with 128 input neurons and a ReLU activation function were used. Then, a batch normalization followed by a dropout with a probability of 0.7 were used (see [23]). Finally, a fully connected layer with 64 input neurons followed by a softmax activation function. In addition, we define a kernel initializer as the glorot uniform and a bias initializer of zeros for initializing the layer's weights throughout the network. This model was also compiled with the Adam optimizer using a learning rate of 2.7×10^{-6} and a binary cross entropy function to measure the performance. The batch size for this model is set to 5 for 50 epochs.

IV. NUMERICAL EXPERIMENTS

In this section, we define the experiments that were conducted using the models described in the previous sections.

Experiment A: Control Normal/Early MCI Classification. In this experiment, we classify images from Control Normal and Early MCI patients along the three different MRI planes: axial, coronal and sagittal. This first experiment classifies between the first two stages leading to dementia. A high performance for this experiment would be crucial for early detection of Alzheimer's disease.

Experiment B: Control Normal/Late MCI Classification. In this experiment, we classify images from Control Normal and Late MCI patients along the three different MRI planes. For this second experiment, there should be a bigger difference between the first stage of the healthy brains and the third stage of LMCI. Therefore, we should expect a noticeable different in the classification for this second experiment.

Experiment C: Early MCI/Late MCI Classification. In this experiment, we classify images from Early MCI and Late MCI patients along the three different MRI planes. In this third experiment, we study the distinction between the early and late stages within the MCI phase.

A. Performance Measurements

The performance of each model will be evaluated using five metrics which use the following values:

- True positive (TP): the total number of positive classifications that are correct;
- True negative (TN): the total number of negative classifications that are correct;
- False positive (FP): the total number of positive classifications that are incorrect;
- False negative (FN): the total number of negative classifications that are incorrect.

The five metrics that we use are as follows:

1) Accuracy: The percentage of the whole sample size that are correctly classified:
$$\text{Accuracy} = \frac{\text{TP} + \text{TN}}{\text{TP} + \text{FP} + \text{TN} + \text{FN}} \times \ 100$$
2) Specificity: The percentage of the total sample that are negative that are correctly classified:
$$\text{Specificity} = \frac{\text{TN}}{\text{TN} + \text{FP}} \times 100$$
3) Recall: The percentage of the total sample that are positive that are correctly classified:
$$\text{Recall (R)} = \frac{\text{TP}}{\text{TP} + \text{FN}} \times 100$$
4) Precision: The percentage of the positive classifications that are correct:
$$\text{Precision (P)} = \frac{\text{TP}}{\text{TP} + \text{FP}} \times 100$$
5) F-score: The harmonic mean of precision and recall:
$$\text{F-score} \ = 2 \times \frac{\text{P} \times \text{R}}{\text{P} + \text{R}} \times 100$$

Experiment A is the binary classification of CN and EMCI, while Experiment B is the binary classification of CN and LMCI. Thus, for Experiments A and B, we define true positive as the number of EMCI or LMCI subjects who were correctly classified. Then, we define true negative as the number of healthy brains correctly classified as CN. The false positive is defined as the number of CNs that are classified as EMCI or LMCI. Finally, the false negative is defined as the number of EMCI or LMCI classified as CNs.

For Experiment C, we define true positive as the number of EMCI correctly classified. Furthermore, true negative is defined as the number of LMCI correctly classified. Then, false positive is the number of LMCIs classified as EMCIs and false negative is defined as the number of EMCIs classified as LMCIs.

V. RESULTS

In this section, we present the results and analyze the three numerical experiments in Sec. IV using the five metrics described previously.

Experiment A: CN/EMCI Classification. The results for this experiment can be found in Table II, where we can see that Model I outperforms Model II in all metrics along the three anatomical planes. Furthermore, in Model I, the coronal plane provides the highest values for all five performance measures, while in Model II, the coronal plane present the highest values in only three out of the five metrics. The highest accuracy values of 78.90% for Model I and 66.69% for Model II were achieved along the coronal plane.

The performance results among Model I are all fairly similar. Along the coronal plane, we have the highest specificity at 79.30%. The specificity reflects how many CN cases were classified correctly. Therefore, the higher the specificity, the fewer normal subjects were classified as EMCI. We also have a relatively high values in recall (78.49%) and precision (79.39%) for the coronal plane, which means our first model is able to detect and discriminate the differences between healthy brains and EMCI better along this plane.

For Model II, the performance results are not as consistent as for Model I. As stated above, only three out of the five metrics rank the highest for the coronal plane. The sagittal plane ranks significantly higher in the other two measures (specificity and precision), which indicates that more images of healthy brains were correctly classified and that among those images labelled as EMCI, a higher percentage was correctly classified. However, the relative low recall value for the sagittal plane indicates that a higher number of false negatives were obtained. This means that a greater number of EMCI brain images were incorrectly classified as healthy, which can have deleterious medical diagnosis consequences.

TABLE II: Experiment A performance measure results for CN/EMCI classification using Simple CNN (Model I) and VoxCNN 2D (Model II) along three different MRI planes.

	MRI Views	**Accur.** (%)	**Spec.** (%)	**Rec.** (%)	**Prec.** (%)	**F-Sc.** (%)
Model I	Axial	76.57	75.27	77.87	75.96	76.86
	Coronal	**78.90**	**79.30**	**78.49**	**79.39**	**78.77**
	Sagittal	77.07	79.05	75.10	78.30	76.58
Model II	Axial	65.85	66.72	64.98	66.47	65.45
	Coronal	**66.69**	66.30	**67.07**	66.61	**66.74**
	Sagittal	66.21	**75.15**	57.27	**70.36**	62.58

Experiment B: CN/LMCI Classification. The results for this experiment can be found in Table III, where we see that Model I outperforms Model II in all metrics along the three anatomical planes. As in Experiment A, the coronal plane shows a higher range in all five metrics for Model I. On the other hand, Model II has a higher range in the coronal plane for three out of five metrics, similar to Experiment A. Additionally, the coronal plane also has higher accuracy compared to the other anatomical planes. The classification of CN and LMCI for the coronal plane results in a high accuracy of 79.67% for Model I compared to the highest accuracy of 67.85% obtained for Model II.

While the performance measures from Model I are similar overall, there are some metrics that are more pronounced than others. The results indicate a relatively very high specificity value of 82.44% for the coronal plane, which indicates that fewer healthy brains were misclassified as LMCI. In addition, among those images that are labelled as LMCI, a relatively very high percentage (81.50%) was correctly classified. The increase in specificity and precision can be attributed to a greater anatomical difference between the first stage of healthy brains to the third stage of LMCI.

As in Experiment A, we see an inconsistency in the performance measures for Model II compared to Model I, and only three out of the five metrics rank the highest for the coronal plane. Model II shows similar results regarding relatively high specificity and precision values for the sagittal plane. Interestingly, there is a slight decrease in these values compared to those in Experiment A, while there are improvements within the other metrics (accuracy, recall, and F-score).

TABLE III: Experiment B performance measure results for CN/LMCI classification using Simple CNN (Model I) and VoxCNN 2D (Model II) along three different MRI planes.

	MRI Views	**Accur.** (%)	**Spec.** (%)	**Rec.** (%)	**Prec.** (%)	**F-Sc.** (%)
Model I	Axial	77.17	80.04	74.30	78.84	76.48
	Coronal	**79.67**	**82.44**	**76.90**	**81.50**	**79.06**
	Sagittal	77.45	79.09	75.81	78.48	77.04
Model II	Axial	67.02	65.58	68.45	66.96	67.16
	Coronal	**67.85**	66.24	**69.47**	67.81	**68.12**
	Sagittal	67.41	**72.71**	62.11	**69.76**	65.38

Experiment C: EMCI/LMCI Classification. The results for this experiment can be found in Table III. Just like Experiments A and B, Model I surpasses Model II for all metrics for all three planes. However, unlike the previous experiments, Model I has a higher value in the coronal plane for four out of five metrics while Model II has a higher range in the coronal plane for all five metrics. Note that the coronal planes has a higher accuracy compared to the axial and sagittal planes for both models.

For Model I, the performance measure values are similar to each other. For the metric where the coronal plane did not provide the highest value (recall), it was a very close second: 77.56% for the coronal plane versus 77.77% for the sagittal plane. For both models overall, the measurement values are lower compared to Experiments A and B. This decline in performance metrics can be attributed to EMCI and LMCI patients having more similar brain image characteristics than for those patients in the other experiments.

TABLE IV: Experiment C performance measure results for EMCI/LMCI classification using Simple CNN (Model I) and VoxCNN 2D (Model II) along three different MRI planes.

	MRI Views	**Accur.** (%)	**Spec.** (%)	**Rec.** (%)	**Prec.** (%)	**F-Sc.** (%)
Model I	Axial	74.36	74.07	74.65	74.27	74.43
	Coronal	**77.02**	**76.47**	77.56	**76.86**	**77.10**
	Sagittal	76.82	75.87	**77.77**	76.49	76.99
Model II	Axial	62.41	61.69	63.14	62.30	62.53
	Coronal	**64.76**	**63.41**	**66.10**	**64.64**	**64.99**
	Sagittal	63.35	62.31	64.40	63.31	63.51

Summary. The results for the dataset considered show that the simpler CNN architecture (Model I) outperforms the more sophisticated CNN (Model II). Additionally, the classification performance improves when comparing images from stages that are farther apart (CN and LMCI). Furthermore, the coronal plane has the highest accuracy between the axial and sagittal planes in all three experiments for both Model I and Model II, while the axial plane had the lowest

percentages for the performance measurements out of the three anatomical planes. We performed the experiments with the assumptions that the dataset acquired characterized a noticeable difference between the baseline of healthy brains and brains diagnosed with MCI. These results tells us that there was less information for the classification of each brain present in the axial slices compared to the coronal and sagittal planes in these experiments.

VI. CONCLUSIONS

The study of mild cognitive impairment is critical for the early diagnosis of Alzheimers disease. Therefore, an accurate and reliable diagnosis of MCI will aid in identifying those individuals at an increased risk of the progression to dementia. In recent years, deep learning has contributed to solving such complex problems. Thus, a convolutional neural network can provide important information to classify between CN, EMCI and LMCI patients.

In this paper, we applied two different classification methods to investigate the performance of two-dimensional MRI images under data quantity limitations. Additionally, we studied the binary classifications of CN, EMCI and LMCI with regard to the three anatomical planes: axial, coronal and sagittal. We performed a thorough analysis to gain insight into what the proposed models had learned. The best results were achieved for the classification of CN and LMCI for the coronal plane. Overall the results indicate that the simpler CNN architecture outperforms a more sophisticated CNN under a limited dataset.

ACKNOWLEDGMENT

We would like to give special acknowledgments to Dr. Omar DeGuchy and Jacqueline Alvarez in the Applied Mathematics Department of the University of California, Merced for their advice and input on this work. We thank Prof. Jennifer Erway for initial conversations on this subject.

REFERENCES

[1] Alzheimer's Association and others, "2018 Alzheimer's disease facts and figures," *Alzheimer's & Dementia*, vol. 14, no. 3, pp. 367–429, 2018.

[2] M. S. Albert, S. T. DeKosky, D. Dickson, B. Dubois, H. H. Feldman, N. C. Fox, A. Gamst, D. M. Holtzman, W. J. Jagust, R. C. Petersen, *et al.*, "The diagnosis of mild cognitive impairment due to Alzheimers disease: recommendations from the National Institute on Aging-Alzheimer's Association workgroups on diagnostic guidelines for Alzheimer's disease," *Focus*, vol. 11, no. 1, pp. 96–106, 2013.

[3] R. C. Petersen, O. Lopez, M. J. Armstrong, T. S. Getchius, M. Ganguli, D. Gloss, G. S. Gronseth, D. Marson, T. Pringsheim, G. S. Day, *et al.*, "Practice guideline update summary: Mild cognitive impairment: Report of the Guideline Development, Dissemination, and Implementation Subcommittee of the American Academy of Neurology," *Neurology*, vol. 90, no. 3, pp. 126–135, 2018.

[4] A. Ward, S. Tardiff, C. Dye, and H. M. Arrighi, "Rate of conversion from prodromal Alzheimer's disease to Alzheimer's dementia: a systematic review of the literature," *Dementia and geriatric cognitive disorders extra*, vol. 3, no. 1, pp. 320–332, 2013.

[5] A. J. Mitchell and M. Shiri-Feshki, "Rate of progression of mild cognitive impairment to dementia–meta-analysis of 41 robust inception cohort studies," *Acta Psychiatrica Scandinavica*, vol. 119, no. 4, pp. 252–265, 2009.

[6] P. Lee, H. Ryoo, J. Park, and Y. Jeong, "Morphological and microstructural changes of the hippocampus in early MCI: a study utilizing the Alzheimer's disease neuroimaging initiative database," *Journal of Clinical Neurology*, vol. 13, no. 2, pp. 144–154, 2017.

[7] J. Escudero, J. P. Zajicek, and E. Ifeachor, "Machine learning classification of MRI features of Alzheimer's disease and mild cognitive impairment subjects to reduce the sample size in clinical trials," in *2011 Annual International Conference of the IEEE Engineering in Medicine and Biology Society*, pp. 7957–7960, IEEE, 2011.

[8] D. Zhang, Y. Wang, L. Zhou, H. Yuan, D. Shen, Alzheimer's Disease Neuroimaging Initiative, *et al.*, "Multimodal classification of Alzheimer's disease and mild cognitive impairment," *Neuroimage*, vol. 55, no. 3, pp. 856–867, 2011.

[9] L. O'Dwyer, F. Lamberton, A. L. Bokde, M. Ewers, Y. O. Faluyi, C. Tanner, B. Mazoyer, D. O'Neill, M. Bartley, D. R. Collins, *et al.*, "Using support vector machines with multiple indices of diffusion for automated classification of mild cognitive impairment," *PloS one*, vol. 7, no. 2, p. e32441, 2012.

[10] E. Challis, P. Hurley, L. Serra, M. Bozzali, S. Oliver, and M. Cercignani, "Gaussian process classification of Alzheimer's disease and mild cognitive impairment from resting-state fmri," *NeuroImage*, vol. 112, pp. 232–243, 2015.

[11] M. Dyrba, F. Barkhof, A. Fellgiebel, M. Filippi, L. Hausner, K. Hauenstein, T. Kirste, S. J. Teipel, and EDSD study group, "Predicting prodromal Alzheimer's disease in subjects with mild cognitive impairment using machine learning classification of multimodal multicenter diffusion-tensor and magnetic resonance imaging data," *Journal of Neuroimaging*, vol. 25, no. 5, pp. 738–747, 2015.

[12] A. Khazaee, A. Ebrahimzadeh, and A. Babajani-Feremi, "Application of advanced machine learning methods on resting-state fMRI network for identification of mild cognitive impairment and Alzheimer's disease," *Brain imaging and behavior*, vol. 10, no. 3, pp. 799–817, 2016.

[13] G. Gosztolya, V. Vincze, L. Tóth, M. Pákáski, J. Kálmán, and I. Hoffmann, "Identifying mild cognitive impairment and mild Alzheimer?s disease based on spontaneous speech using asr and linguistic features," *Computer Speech & Language*, vol. 53, pp. 181–197, 2019.

[14] S. O. Orimaye, K. Goodkin, O. A. Riaz, J.-M. M. Salcedo, T. Al-Khateeb, A. O. Awujoola, and P. O. Sodeke, "A machine learning-based linguistic battery for diagnosing mild cognitive impairment due to Alzheimer?s disease," *Plos one*, vol. 15, no. 3, p. e0229460, 2020.

[15] E. Pellegrini, L. Ballerini, M. d. C. V. Hernandez, F. M. Chappell, V. González-Castro, D. Anblagan, S. Danso, S. Muñoz-Maniega, D. Job, C. Pernet, *et al.*, "Machine learning of neuroimaging for assisted diagnosis of cognitive impairment and dementia: a systematic review," *Alzheimer's & Dementia: Diagnosis, Assessment & Disease Monitoring*, vol. 10, pp. 519–535, 2018.

[16] H. Taheri Gorji and N. Kaabouch, "A deep learning approach for diagnosis of mild cognitive impairment based on MRI images," *Brain sciences*, vol. 9, no. 9, p. 217, 2019.

[17] S. Korolev, A. Safiullin, M. Belyaev, and Y. Dodonova, "Residual and plain convolutional neural networks for 3D brain MRI classification," in *2017 IEEE 14th International Symposium on Biomedical Imaging (ISBI 2017)*, pp. 835–838, IEEE, 2017.

[18] A. Mehmood, M. Maqsood, M. Bashir, and Y. Shuyuan, "A deep siamese convolution neural network for multi-class classification of Alzheimer disease," *Brain Sciences*, vol. 10, no. 2, p. 84, 2020.

[19] P. Forouzannezhad, A. Abbaspour, C. Li, M. Cabrerizo, and M. Adjouadi, "A deep neural network approach for early diagnosis of mild cognitive impairment using multiple features," in *2018 17th IEEE International Conference on Machine Learning and Applications (ICMLA)*, pp. 1341–1346, IEEE, 2018.

[20] J. Ashburner, G. Barnes, C. Chen, J. Daunizeau, G. Flandin, K. Friston, S. Kiebel, J. Kilner, V. Litvak, R. Moran, *et al.*, "SPM12 manual," *Wellcome Trust Centre for Neuroimaging, London, UK*, p. 2464, 2014.

[21] Y. Zhang, N. Schuff, M. Camacho, L. L. Chao, T. P. Fletcher, K. Yaffe, S. C. Woolley, C. Madison, H. J. Rosen, B. L. Miller, *et al.*, "Mri markers for mild cognitive impairment: comparisons between white matter integrity and gray matter volume measurements," *PloS one*, vol. 8, no. 6, p. e66367, 2013.

[22] D. P. Kingma and J. Ba, "Adam: A method for stochastic optimization," *arXiv preprint arXiv:1412.6980*, 2014.

[23] N. Srivastava, G. Hinton, A. Krizhevsky, I. Sutskever, and R. Salakhutdinov, "Dropout: a simple way to prevent neural networks from overfitting," *The Journal of Machine Learning Research*, vol. 15, no. 1, pp. 1929–1958, 2014.